

# Enhanced Nonlinear Optical Responses of Layered Epsilon-near-Zero Metamaterials at Visible Frequencies

Sisira Suresh, Orad Reshef,\* M. Zahirul Alam, Jeremy Upham, Mohammad Karimi, and Robert W. Boyd



Cite This: *ACS Photonics* 2021, 8, 125–129



Read Online

ACCESS |

Metrics & More

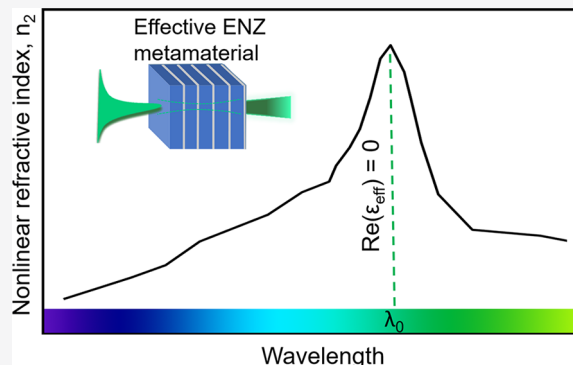
Article Recommendations

Supporting Information

**ABSTRACT:** Optical materials with vanishing dielectric permittivity, known as epsilon-near-zero (ENZ) materials, have been shown to possess enhanced nonlinear optical responses in their ENZ region. These strong nonlinear optical properties have been firmly established in homogeneous materials; however, it is as of yet unclear whether metamaterials with effective optical parameters can exhibit a similar enhancement. Here, we probe an optical ENZ metamaterial composed of a subwavelength periodic stack of alternating Ag and  $\text{SiO}_2$  layers and measure a nonlinear refractive index  $n_2 = (1.2 \pm 0.1) \times 10^{-12} \text{ m}^2/\text{W}$  and nonlinear absorption coefficient  $\beta = (-1.5 \pm 0.2) \times 10^{-5} \text{ m}/\text{W}$  at its effective zero-permittivity wavelength. The measured  $n_2$  is  $10^7$  times larger than  $n_2$  of fused silica and 4 times larger than the  $n_2$  of silver. We observe that the nonlinear enhancement in  $n_2$  scales as  $1/(n_0 \text{Re}[n_0])$ , where  $n_0$  is the linear effective refractive index. As opposed to homogeneous ENZ materials, whose optical properties are dictated by their intrinsic material properties and hence are not widely tunable, the zero-permittivity wavelength of the demonstrated metamaterials may be chosen to lie anywhere within the visible spectrum by selecting the right thicknesses of the subwavelength layers. Consequently, our results offer the promise of a means to design metamaterials with large nonlinearities for applications in nanophotonics at any specified optical wavelength.

**KEYWORDS:** *epsilon-near-zero, metamaterials, nonlinear optics, multilayer stack, nanophotonics*

In recent years, much attention has been given to a class of materials with vanishing dielectric permittivity.<sup>1–3</sup> This class of materials, known as epsilon-near-zero (ENZ) materials, has become a topic of interest because of its intriguing optical properties including tunneling of light through arbitrary bends,<sup>1</sup> the ability to tailor radiation patterns,<sup>4</sup> and its enhanced nonlinear optical response.<sup>5–8</sup> The ENZ condition can be found in naturally occurring materials near their bulk plasma and phonon resonances. Most noble metals exhibit a zero-permittivity behavior in the UV region, near their respective plasma frequencies.<sup>9</sup> Transition metal nitrides such as titanium nitride<sup>10</sup> and zirconium nitride<sup>11</sup> display their ENZ regime in the visible spectral region. In the near-infrared (NIR) region, doped semiconducting oxides such as tin-doped indium oxide<sup>12</sup> and aluminum-doped zinc oxide<sup>13</sup> behave as ENZ materials. An ENZ condition is also found in silicon carbide,<sup>14</sup> the perovskite strontium titanate,<sup>15</sup> gallium nitride,<sup>16</sup> and fused silica ( $\text{SiO}_2$ )<sup>17</sup> in the mid-IR range due to phononic resonances. The zero-permittivity wavelength of a given material is dictated by its intrinsic material properties and hence cannot be used for applications that require that the ENZ condition occurs at some specified wavelength. To address this concern, ENZ metamaterials have been developed for use in the microwave,<sup>18</sup> IR,<sup>2,19</sup> and visible<sup>20,21</sup> spectral regions. In homogeneous Drude materials, the nonlinear



enhancement of  $n_2$  and  $\beta$  has been thoroughly examined as a function of wavelength in the ENZ region.<sup>8</sup> Although some work has been done exploring the nonlinear response of ENZ metamaterials,<sup>22–24</sup> its dependence as a function of wavelength has yet to be fully characterized. Doing this allows us to implicitly infer  $n_2$  as a function of  $\epsilon$  and, thus, interpret the ENZ condition's real contribution to the optical nonlinearity. Here, we examine the nonlinear optical response of an ENZ metamaterial that is straightforward to fabricate and for which the ENZ condition can be flexibly set to any targeted wavelength region. Although the nonlinear enhancement in homogeneous ENZ materials has been well established, it is not clear whether such an enhancement occurs in metamaterials when the *effective* permittivity vanishes. In homogeneous materials such as tin-doped indium oxide, the nonlinear enhancement can be explained by a shift in the plasma frequency by intense laser excitation, which changes the

Received: July 27, 2020

Published: December 11, 2020



permittivity.<sup>12</sup> The refractive index then changes according to  $\Delta n = \Delta\epsilon/2\sqrt{\epsilon}$ , which has its maximum value at the zero-permittivity wavelength. It has yet to be established whether  $\Delta n$  is maximally changed at the effective zero-permittivity wavelength of a metamaterial. Our work confirms that a metamaterial indeed does exhibit a nonlinear enhancement in its ENZ region, and therefore, ENZ nonlinear enhancement can be placed at any predefined wavelength. We also develop a simple analytic model to explain these results.

Our metamaterial is composed of alternating subwavelength-thick layers of metal and dielectric materials. A schematic diagram of the metamaterial geometry is shown in Figure 1(a). A

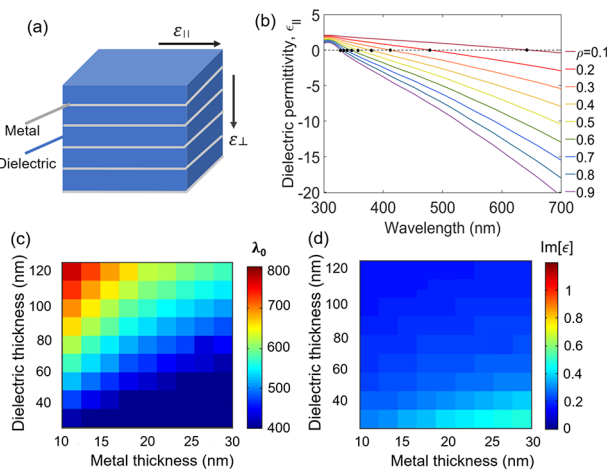


**Figure 1.** (a) Schematic diagram of a metal–dielectric multilayer stack. (b) Effective parallel permittivities at normal incidence predicted from EMT for different metallic fill fractions (the black circles denote the zero-crossing wavelength for each fill fraction). (c) The zero-permittivity wavelength and (d) the loss of a five-bilayer Ag–SiO<sub>2</sub> multilayer stack calculated using TMM as a function of the thicknesses of the Ag and SiO<sub>2</sub> layers. Note that the zero-permittivity wavelength can be placed anywhere in the visible region.

These metamaterials are capable of exhibiting a zero-permittivity wavelength anywhere within the entire visible spectrum by adjusting the respective thicknesses of the constituent materials.<sup>20,25–27</sup> Provided that the inhomogeneity scale of the composite medium is of subwavelength dimensions, effective medium theory (EMT) predicts that the wavelength,  $\lambda_0$ , at which the permittivity crosses zero can be evaluated from the fill fraction of the constituents in the composite.<sup>25,28</sup> Thus, in the limit of subwavelength layer thickness, the metal–dielectric multilayer stack can be considered as an effective medium with an effective permittivity for an electric field polarized in the plane of the layers given by  $\epsilon_{||} = \rho\epsilon_m + (1 - \rho)\epsilon_d$ , where  $\rho$  is the metallic fill fraction and  $\epsilon_m$  and  $\epsilon_d$  are the permittivities of the metal and the dielectric material, respectively.<sup>29</sup> We selected Ag as the metal because of its small damping constant compared to other noble metals,<sup>30</sup> and SiO<sub>2</sub> as the dielectric because of its transparency in the visible spectral region.<sup>31</sup> In Figure 1(b), the fill fraction is varied from  $\rho = 0.1$  to  $0.9$ , and we observe a blue shift in the zero-permittivity wavelength as the metallic fill fraction increases. Thus, the dependence of the zero-permittivity wavelength on the metallic fill fraction should enable an ENZ metamaterial design that can be situated anywhere in the entire visible spectrum.

Although effective medium theory can reliably predict the ENZ wavelength under many situations, this method is rigorously valid only under limiting conditions, such as vanishingly small layer thickness and an infinitely thick overall medium.<sup>32</sup> In order to validate our EMT approach, we perform parameter retrieval using the transfer matrix method (TMM) to aid in our design.<sup>33</sup> Using this method, one can solve for the effective refractive index and consequently the complex effective permittivity of a medium. The TMM simulations reveal optimal designs in terms of zero-permittivity wavelength and optical losses (Figure 1(c)). We select a design for the Ag–SiO<sub>2</sub> multilayer stack that has both a desired zero-permittivity wavelength and a small amount of loss, consisting of five bilayers of Ag and SiO<sub>2</sub> with thicknesses of 16 and 65 nm, respectively, for a total thickness of 405 nm. We choose five bilayers because it has been shown that using more than five bilayers produces no appreciable improvement in the nonlinear optical response.<sup>47</sup> Figure 2(a) depicts the dielectric

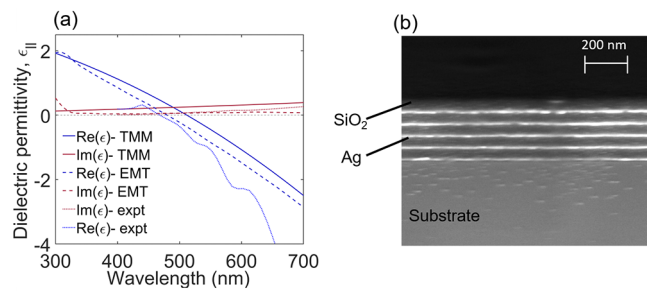


**Figure 2.** (a) Effective parallel permittivity,  $\epsilon_{||}$ , at normal incidence calculated using the TMM, EMT, and the measured transmittance for a Ag–SiO<sub>2</sub> multilayer stack with five bilayers of Ag (16 nm) and SiO<sub>2</sub> (65 nm). (b) Cross-sectional image of the fabricated Ag–SiO<sub>2</sub> multilayer stack taken with a scanning electron microscope.

permittivity at normal incidence as a function of wavelength calculated using both the TMM and EMT methods. The optical losses are due to the resistive losses of silver. This geometry corresponds to a metamaterial with an effective zero-permittivity wavelength of 509 nm, with an imaginary part of the dielectric permittivity  $\text{Im}[\epsilon]$  of 0.2.

Having established a preferred design, we fabricated a device for characterization. The Ag and SiO<sub>2</sub> layers were deposited using electron-beam evaporation on a glass substrate. The deposition rates of Ag and SiO<sub>2</sub> layers were kept at a low value of 0.1 nm/s in order to maintain film uniformity. To prevent oxidation, the top layer is the SiO<sub>2</sub> layer. A cross-section of the fabricated sample is shown in Figure 2(b). Our fabricated sample agrees with our design within the usual fabrication tolerances.

## METHODS

The linear transmittance of the sample was probed using a collimated supercontinuum source covering the visible to NIR spectral range. We compared the measured transmission spectra to those predicted by TMM simulations for various metal and dielectric layer thicknesses. We found the best agreement with the experimental data for a metal–dielectric multilayer stack with thicknesses of 16 nm for Ag and 56 nm for SiO<sub>2</sub> (see Supporting Information for more details). The resulting zero-permittivity wavelength occurs at 470 nm (Figure 2(a)), which is reasonably close to the predicted

zero-permittivity wavelength of our device design (509 nm). The small discrepancy between the target zero-crossing wavelength and that determined from these linear characterization measurements could be attributable to fabrication uncertainties, such as layer composition or variations in thickness, or measurement uncertainties in the linear characterization of the device.

We characterized the nonlinear optical properties of our sample using the Z-scan technique.<sup>34</sup> A schematic diagram of the experimental setup is shown in Figure 3(a). We used pump

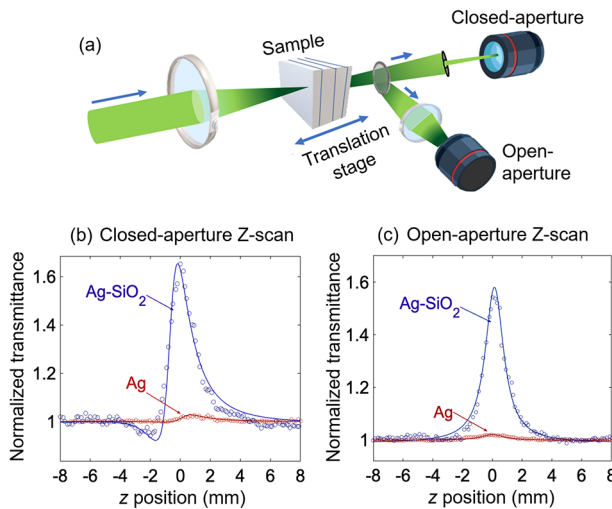


**Figure 3.** (a) Experimental setup. The Z-scan measurements were performed using 28 ps pulses with a repetition rate of 50 Hz from an optical parametric generator. A spatially filtered Gaussian beam is focused at normal incidence onto the sample by a lens. (b) Closed- and (c) open-aperture Z-scan signals at  $\lambda = 500$  nm for a Ag–SiO<sub>2</sub> multilayer stack (blue) and a thin-film Ag layer (red) at normal incidence. The solid lines represent theoretical fits to the experimental data.

pulses with a repetition rate of 50 Hz and a pulse duration of 28 ps from an optical parametric generator. Both closed- and open-aperture measurements were performed for wavelengths ranging from 410 to 560 nm. Note that the entire spectral range is in the ENZ region. All the measurements were conducted at normal incidence. As such, we do not expect to excite any surface plasmon polaritons. Figure 3(b) and (c) show, respectively, representative closed-aperture and open-aperture signals from the Ag–SiO<sub>2</sub> multilayer stack at  $\lambda = 500$  nm. The asymmetry in the closed-aperture signal with respect to the focus is due to the significant nonlinear absorption in the sample.<sup>35,36</sup> We first extracted the imaginary part of the nonlinear phase shift from the open-aperture signal and used this value to calculate the real part of the phase shift from the closed-aperture signal. The extracted values of the real and imaginary nonlinear phase shifts were used in the standard expressions to calculate  $n_2$  and  $\beta$  (see Supporting Information for details).<sup>34</sup> For comparison, Figure 3(b) and (c) also show similar measurements performed under the same conditions for a single 16-nm-thick Ag layer. Near the zero-permittivity wavelength, the accumulated nonlinear phase of the multilayer stack is 22 times larger than that of the 16-nm-thick silver layer, even though the multilayer stack contains only 5 times as much silver.

The nonlinear refractive index  $n_2$  and the nonlinear absorption coefficient  $\beta$  of the Ag–SiO<sub>2</sub> multilayer stack are shown as functions of wavelength in Figure 4(a) and (b). It is

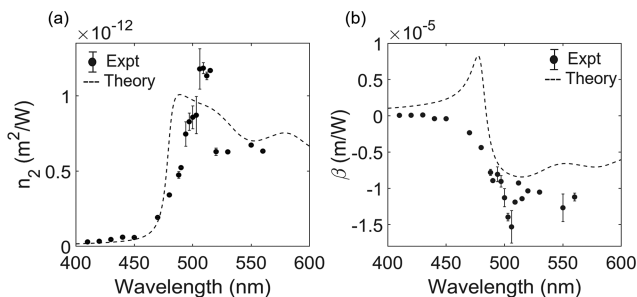


**Figure 4.** (a) Nonlinear refractive index  $n_2$  and (b) nonlinear absorption coefficient  $\beta$  of the Ag–SiO<sub>2</sub> multilayer stack as a function of wavelength. The dashed lines correspond to predictions from eqs 2 and 3 without any fit parameters.

clear that the nonlinear response is enhanced in the ENZ region of the spectrum, peaking at the zero-permittivity wavelength targeted by this metamaterial design. The maximum measured phase shift at the zero-permittivity wavelength is  $0.62\pi \pm 0.05$  rad. For the Ag–SiO<sub>2</sub> multilayer stack, the values of  $n_2$  and  $\beta$  are  $(1.2 \pm 0.1) \times 10^{-12} \text{ m}^2/\text{W}$  and  $(-1.5 \pm 0.2) \times 10^{-5} \text{ m}/\text{W}$ , respectively. The peak value of the measured  $n_2$  of the Ag–SiO<sub>2</sub> multilayer stack is  $10^7$  times larger than that of fused silica ( $3.2 \times 10^{-20} \text{ m}^2/\text{W}$ )<sup>38</sup> and is 4 times larger than that of an individual 16-nm-thick silver film ( $3 \times 10^{-13} \text{ m}^2/\text{W}$ ). Due to the noninstantaneous nature of the nonlinearity of metals, we would expect to obtain different values for the nonlinear response for different experimental conditions. For example, we expect that performing the same measurements as reported above with shorter pulses would lead to smaller magnitudes of nonlinearity.<sup>37</sup> However, by performing our measurement with a narrow-band pulse, we are able to measure the nonlinear response across a broad spectral range spanning over the ENZ wavelength for this sample, confirming the existence of clear nonlinear enhancement due to the zero-permittivity wavelength.

## RESULTS AND DISCUSSION

We model the nonlinearity of the metamaterial stack using the nonlinear EMT.<sup>39</sup> Here, the effective nonlinear susceptibility of the metamaterial stack is the weighted average of the constituent materials. Since  $\chi_{\text{SiO}_2}^{(3)}$  is much smaller than  $\chi_{\text{Ag}}^{(3)}$ , according to EMT, the dominant contribution to  $\chi_{\text{eff}}^{(3)}$  of the metamaterial is from the Ag layers only (e.g.,  $\chi_{\text{eff}}^{(3)} \approx \chi_{\text{Ag}}^{(3)} \times \rho$ ). We assume that  $\chi_{\text{Ag}}^{(3)}$  is dispersionless over this spectral range. We measured our single silver layer sample at  $\lambda = 500$  nm and obtained  $\chi^{(3)} = (2.42 + 5.15i) \times 10^{-16} \text{ m}^2/\text{V}^2$ , in good agreement with previously measured values.<sup>40,41</sup> The complex nonlinear response  $\tilde{n}_2$  of the composite material is given by<sup>38,42,43</sup>

$$\tilde{n}_2 = \frac{3}{4\epsilon_0 cn_0 \text{Re}[n_0]} \chi_{\text{eff}}^{(3)} \quad (1)$$

where  $\epsilon_0$  is the vacuum permittivity and  $c$  is the speed of light in a vacuum. Equation 1 is related to the nonlinear refraction  $n_2$  and the absorption coefficient  $\beta$  by the relations

$$n_2 = \text{Re}[\tilde{n}_2] \quad (2)$$

$$\beta = \frac{4\pi}{\lambda} \text{Im}[\tilde{n}_2] \quad (3)$$

We plot these equations in **Figure 4** using the refractive index of our design as calculated by the EMT. The model shows a strong, wavelength-dependent enhancement at the zero-permittivity wavelength that qualitatively resembles the experimental results. It correctly predicts the location and the maximum nonlinear response to within a factor of 2 without the need for any fit parameters or additional factors (e.g., the slow-light factor  $S = n_g/n_0$ , where  $n_g$  is the group index<sup>44,45</sup>). The discrepancies in the breadth and the magnitude of this enhancement at the peak could likely be attributed to dimension variations between the design and the fabricated device, surface effects, imperfections in the constituent layers introduced during deposition, or our assumption that  $\chi_{\text{Ag}}^{(3)}$  is dispersionless in our theoretical model. We note that our model predicts an additional peak for  $\beta$  at  $\lambda = 475$  nm that we do not reproduce in the measurement and currently cannot account for. The qualitative agreement between such a simple theory and the experimental results suggests that this model may be used to predict and design the nonlinear optical response of other ENZ metamaterials.

In order to study the nature of the enhancement of the nonlinear response, we compare the response of the Ag–SiO<sub>2</sub> multilayer stack directly with that of a single thin film of silver. Given that  $\chi_{\text{eff}}^{(3)} \approx \rho \times \chi_{\text{Ag}}^{(3)}$ , with  $\rho < 1$ , any metamaterial stack composed of SiO<sub>2</sub> and Ag layers will exhibit a smaller  $\chi^{(3)}$  value than that of silver. However, we found that at its peak the magnitude of  $n_2$  of the metamaterial is 4 times that of silver. This observation implies that the ENZ condition increases  $n_2$  to exceed the value of silver, despite the silver being “diluted” by a material with a lower nonlinearity (i.e., SiO<sub>2</sub>). This observation is further validated when comparing  $n_2$  and  $\beta$  of the ENZ metamaterial at its zero-permittivity wavelength ( $\lambda = 506$  nm) to these same values when  $\epsilon_{\text{eff}} \approx 1$  ( $\lambda = 410$  nm; see **Figure 2(a)**). Here, the magnitudes of  $n_2$  and  $\beta$  are increased in the ENZ region by factors of 40 and 250, respectively. In addition to this ENZ enhancement, at the zero-permittivity wavelength, the metamaterial has a smaller linear loss than silver ( $\text{Im}[n_0] = 0.3$  vs 3.1, respectively). Consequently, its effective propagation length can be much longer than that of silver (60 nm vs 9 nm), allowing for a much larger accumulation of nonlinear phase.<sup>46,47</sup> As shown by the peak-to-valley differences in **Figure 3(b)**, in propagating through a five-bilayer Ag–SiO<sub>2</sub> multilayer stack, the beam acquires a nonlinear phase shift that is approximately 22 times larger than that of the individual silver layer (1.53 rad vs 0.068 rad). Therefore, the benefit of using an ENZ metamaterial over a bulk metallic thin film is twofold: due to ENZ enhancement and due to lowered loss.<sup>22,24,46,47</sup>

In conclusion, we have examined the nonlinear optical properties of an ENZ metamaterial realized through the use of a metal–dielectric multilayer stack. This work further confirms that the enhancement of the nonlinear optical response that had previously been observed in homogeneous materials at the zero-permittivity wavelength<sup>12,13</sup> occurs also in metamaterials at the zero of the *effective* permittivity.<sup>22–24</sup> We have observed that these materials produce a large nonlinear optical response and that the dominant mechanism for enhancing this response is the factor  $1/(n_0 \text{Re}[n_0])$ . The ability to obtain strong nonlinearities at designated optical frequencies makes these

metamaterials a flexible platform for applications in nonlinear optics.

There exists a broad variety of nonlinear optical phenomena, of which only the Kerr effect and saturable absorption were directly examined in this work. The investigation of other such nonlinear responses<sup>48,49</sup> and their potential enhancement in ENZ metamaterials certainly warrants further study. The fact that this metamaterial geometry is inherently anisotropic could be seen as an advantage for certain future applications and be the topic of future study.

## ASSOCIATED CONTENT

### Supporting Information

The Supporting Information is available free of charge at <https://pubs.acs.org/doi/10.1021/acsphtronics.0c01178>.

Linear characterization methods, beam cleaning procedures, retrieval of nonlinear optical coefficients, peculiar features of open- and closed-aperture Z-scan signals, nonlinear phase shift, and additional experimental details ([PDF](#))

## AUTHOR INFORMATION

### Corresponding Author

Orad Reshef – Department of Physics, University of Ottawa, Ottawa, ON K1N 6NS, Canada;  [orcid.org/0000-0001-9818-8491](https://orcid.org/0000-0001-9818-8491); Email: [orad@reshef.ca](mailto:orad@reshef.ca)

### Authors

Sisira Suresh – Department of Physics, University of Ottawa, Ottawa, ON K1N 6NS, Canada

M. Zahirul Alam – Department of Physics, University of Ottawa, Ottawa, ON K1N 6NS, Canada

Jeremy Upham – Department of Physics, University of Ottawa, Ottawa, ON K1N 6NS, Canada

Mohammad Karimi – School of Electrical Engineering and Computer Science, University of Ottawa, Ottawa, ON K1N 6NS, Canada

Robert W. Boyd – Department of Physics, University of Ottawa, Ottawa, ON K1N 6NS, Canada; Institute of Optics and Department of Physics and Astronomy, University of Rochester, Rochester, New York 14627, United States

Complete contact information is available at:  
<https://pubs.acs.org/10.1021/acsphtronics.0c01178>

### Notes

The authors declare no competing financial interest.

## ACKNOWLEDGMENTS

This work was supported in part by the Canada First Research Excellence Fund, the Canada Research Chairs Program, and the Natural Sciences and Engineering Research Council of Canada (NSERC [funding reference number RGPIN/2017-06880]). R.W.B. acknowledges support from DARPA (Grant No. W911NF-18-0369) and ARO (Grant W911NF-18-1-0337). O.R. acknowledges the support of the Banting Postdoctoral Fellowship from NSERC. Fabrication in this work was performed at the Centre for Research in Photonics at the University of Ottawa (CRPuO).

## ■ REFERENCES

- (1) Silveirinha, M.; Engheta, N. Tunneling of electromagnetic energy through subwavelength channels and bends using  $\epsilon$ -near-zero materials. *Phys. Rev. Lett.* **2006**, *97*, 157403.
- (2) Adams, D. C.; et al. Funneling Light through a Subwavelength Aperture with Epsilon-Near-Zero Materials. *Phys. Rev. Lett.* **2011**, *107*, 133901.
- (3) Prain, A.; Vezzoli, S.; Westerberg, N.; Roger, T.; Faccio, D. Spontaneous Photon Production in Time-Dependent Epsilon-Near-Zero Materials. *Phys. Rev. Lett.* **2017**, *118*, 133904.
- (4) Alù, A.; Silveirinha, M.; Salandrino, A.; Engheta, N. Epsilon-near-zero metamaterials and electromagnetic sources: Tailoring the radiation phase pattern. *Phys. Rev. B: Condens. Matter Mater. Phys.* **2007**, *75*, 155410.
- (5) Ciattoni, A.; Rizza, C.; Palange, E. Transmissivity directional hysteresis of a nonlinear metamaterial slab with very small linear permittivity. *Opt. Lett.* **2010**, *35*, 2130.
- (6) Argyropoulos, C.; Chen, P.; D'Aguanno, G.; Engheta, N.; Alù, A. Boosting optical nonlinearities in epsilon-near-zero plasmonic channels. *Phys. Rev. B: Condens. Matter Mater. Phys.* **2012**, *85*, 045129.
- (7) Capretti, A.; Wang, Y.; Engheta, N.; Dal Negro, L. Enhanced third-harmonic generation in Si-compatible epsilon-near-zero indium tin oxide nanolayers. *Opt. Lett.* **2015**, *40*, 1500–1503.
- (8) Reshef, O.; De Leon, I.; Alam, M. Z.; Boyd, R. W. Nonlinear optical effects in epsilon-near-zero media. *Nature Reviews Materials* **2019**, *4*, 535–551.
- (9) Johnson, P. B.; Christy, R. W. Optical Constants of the Noble Metals. *Phys. Rev. B* **1972**, *6*, 4370–4379.
- (10) Wen, X.; et al. Doubly Enhanced Second Harmonic Generation through Structural and Epsilon-near-Zero Resonances in TiN Nanostructures. *ACS Photonics* **2018**, *5*, 2087–2093.
- (11) Naik, G. V.; Kim, J.; Boltasseva, A. Oxides and nitrides as alternative plasmonic materials in the optical range. *Opt. Mater. Express* **2011**, *1*, 1090–1099.
- (12) Alam, M. Z.; De Leon, I.; Boyd, R. W. Large optical nonlinearity of indium tin oxide in its epsilon-near-zero region. *Science* **2016**, *352*, 795–797.
- (13) Caspani, L.; et al. Enhanced nonlinear refractive index in epsilon-near-zero materials. *Phys. Rev. Lett.* **2016**, *116*, 233901.
- (14) Spitzer, W. G.; Kleinman, D.; Walsh, D. Infrared properties of hexagonal silicon carbide. *Phys. Rev.* **1959**, *113*, 127–132.
- (15) Kehr, S. C.; et al. Near-field examination of perovskite-based superlenses and superlens-enhanced probe-object coupling. *Nat. Commun.* **2011**, *2*, 1–9.
- (16) Harima, H.; Sakashita, H.; Nakashima, S. Raman microprobe measurement of under-damped LO-phonon-plasmon coupled mode in n-type GaN. *Mater. Sci. Forum* **1998**, *264*, 1363–1366.
- (17) Kischkat, J.; et al. Mid-infrared optical properties of thin films of aluminum oxide, titanium dioxide, silicon dioxide, aluminum nitride, and silicon nitride. *Appl. Opt.* **2012**, *51*, 6789–6798.
- (18) Edwards, B.; Alù, A.; Young, M. E.; Silveirinha, M.; Engheta, N. Experimental verification of epsilon-near-zero metamaterial coupling and energy squeezing using a microwave waveguide. *Phys. Rev. Lett.* **2008**, *100*, 033903.
- (19) Hu, C.; et al. Experimental demonstration of near-infrared epsilon-near-zero multilayer metamaterial slabs. *Opt. Express* **2013**, *21*, 23631–23639.
- (20) Subramania, G.; Fischer, A. J.; Luk, T. S. Optical properties of metal-dielectric based epsilon near zero metamaterials. *Appl. Phys. Lett.* **2012**, *101*, 241107.
- (21) Maas, R.; Parsons, J.; Engheta, N.; Polman, A. Experimental realization of an epsilon-near-zero metamaterial at visible wavelengths. *Nat. Photonics* **2013**, *7*, 907912.
- (22) Neira, A. D.; et al. Eliminating material constraints for nonlinearity with plasmonic metamaterials. *Nat. Commun.* **2015**, *6*, 7757.
- (23) Kaipurath, R. M.; et al. Optically induced metal-to-dielectric transition in Epsilon-Near-Zero metamaterials. *Sci. Rep.* **2016**, *6*, 27700.
- (24) Rashed, A. R.; Yildiz, B. C.; Ayyagari, S. R.; Caglayan, H. Hot Electron Dynamics in Ultrafast Multilayer Epsilon-Near-Zero Metamaterial. *Phys. Rev. B: Condens. Matter Mater. Phys.* **2020**, *101*, 165301.
- (25) Wenshan, C.; Shalaev, V. *Optical Metamaterials*; Springer: New York, 2010; p 10.
- (26) Kidwai, O.; Zhukovsky, S. V.; Sipe, J. E. Effective-medium approach to planar multilayer hyperbolic metamaterials: Strengths and limitations. *Phys. Rev. A: At., Mol., Opt. Phys.* **2012**, *85*, 053842.
- (27) Newman, W. D.; et al. Ferrell-berreman modes in plasmonic epsilon-near-zero media. *ACS Photonics* **2015**, *2*, 2–7.
- (28) Sihvola, A. H. *Electromagnetic Mixing Formulae and Applications*; IET, 1999; Vol. 47.
- (29) Rylov, S. M. Electromagnetic Properties of a Finely Stratified Medium. *Sov. Phys. Japt* **1956**, *2*, 466–475.
- (30) West, P. R.; et al. Searching for better plasmonic materials. *Laser and Photonics Reviews* **2010**, *4*, 795–808.
- (31) Palik, E. D. *Handbook of Optical Constants of Solids*; Academic Press, 1998; Vol. 3.
- (32) Papadakis, G. T.; Yeh, P.; Atwater, H. A. Retrieval of material parameters for uniaxial metamaterials. *Phys. Rev. B: Condens. Matter Mater. Phys.* **2015**, *91*, 155406.
- (33) Smith, D. R.; Vier, D. C.; Koschny, T.; Soukoulis, C. M. Electromagnetic parameter retrieval from inhomogeneous metamaterials. *Phys. Rev. E* **2005**, *71*, 036617.
- (34) Sheik-Bahae, M.; Said, A. A.; Wei, T. H.; Hagan, D. J.; Van Stryland, E. W. Sensitive measurement of optical nonlinearities using a single beam. *IEEE J. Quantum Electron.* **1990**, *26*, 760–769.
- (35) Liu, X.; Guo, S.; Wang, H.; Hou, L. Theoretical study on the closed-aperture Z -scan curves in the materials with nonlinear refraction and strong nonlinear absorption. *Opt. Commun.* **2001**, *197*, 431–437.
- (36) Tsigaridas, G.; Persephonis, P.; Giannetas, V. Effects of nonlinear absorption on the Z-scan technique through beam dimension measurements. *Mater. Sci. Eng., B* **2009**, *165*, 182–185.
- (37) Boyd, R. W.; Shi, Z.; De Leon, I. The third-order nonlinear optical susceptibility of gold. *Opt. Commun.* **2014**, *326*, 74–79.
- (38) Boyd, R. W. *Nonlinear Optics*, 4th ed.; Academic Press, 2020.
- (39) Boyd, R. W.; Sipe, J. E. Nonlinear optical susceptibilities of layered composite materials. *J. Opt. Soc. Am. B* **1994**, *11*, 297–303.
- (40) Ma, G.; Tang, S. H. Ultrafast optical nonlinearity enhancement in metalodielectric multilayer stacks. *Opt. Lett.* **2007**, *32*, 3435–3437.
- (41) Yang, G.; Guan, D.; Wang, W.; Wu, W.; Chen, Z. The inherent optical nonlinearities of thin silver films. *Opt. Mater.* **2004**, *25*, 439–443.
- (42) Sutherland, R. L. *Handbook of Nonlinear Optics*; CRC Press, 2003.
- (43) Del Coso, R.; Solis, J. Relation between nonlinear refractive index and third-order susceptibility in absorbing media. *J. Opt. Soc. Am. B* **2004**, *21*, 640–644.
- (44) Monat, C.; De Sterke, M.; Eggleton, B. J. Slow light enhanced nonlinear optics in periodic structures. *J. Opt.* **2010**, *12*, 104003.
- (45) Boyd, R. W. Material slow light and structural slow light: similarities and differences for nonlinear optics. *J. Opt. Soc. Am. B* **2011**, *28*, A38–A44.
- (46) Bennink, R. S.; Yoon, Y.; Boyd, R. W.; Sipe, J. E. Accessing the optical nonlinearity of metals with metal-dielectric photonic bandgap structures. *Opt. Lett.* **1999**, *24*, 1416–1418.
- (47) Lepeshkin, N. N.; Schweinsberg, A.; Piredda, G.; Bennink, R. S.; Boyd, R. W. Enhanced nonlinear optical response of one-dimensional metal-dielectric photonic crystals. *Phys. Rev. Lett.* **2004**, *93*, 123902.
- (48) Luk, T. S.; et al. Enhanced third harmonic generation from the epsilon-near-zero modes of ultrathin films. *Appl. Phys. Lett.* **2015**, *106*, 151103.
- (49) Yang, Y.; et al. High-harmonic generation from an epsilon-near-zero material. *Nat. Phys.* **2019**, *15*, 1022–1026.